PROC. OF JSCE,
No. 325, Sept. 1982

SPATIAL CONSIDERATIONS OF THERMAL BUCKLING OF RAILROAD TRACKS

By Cheng-Ping CHEN and Masahiro KAWAGUCHI***

1. INTRODUCTION

Thermal buckling of rails is an old problem existed since the adoption of rails in railways. Normally, expandable joints are set between members of rail strings to eliminate the constrained thermal axial force in the rails due to seasonal and daily temperature changes. However, the existence of expandable joint itself is the main factor which restricts the train speed, increases the maintenance costs of the track and the trains and also creates noise and some other unfavorable facts. Therefore it has been a desire for railroad engineers to eliminate some of the joints by increasing the length of the rails. For high speed trains the continuously welded track is a necessity. However, the complete elimination of joints increases the possibility of track buckling during the summer. This is the reason that the problem of thermal buckling of rails has become more interesting and important for the engineers today.

Since the problem of rail buckling attracted engineer's attention several decades ago it has been studied by numerous investigators. M. Numata[12] and A. D. Kerr[5~10] gave broad reviews of the researches on this topic. Generally speaking, the published analyses on track buckling may be divided into two groups[6]. In one group the authors assume that the track buckles in the vertical plane, in the other group it is assumed that the track buckles in the horizontal plane. Although the mode of track deformation caused by buckling may be spatial, these assumptions were suggested by observations on buckled tracks and were apparently made to simplify the analysis.

The first field test in Japan was done by I. Horikoshi in 1932[2] and all of the rails buckled finally in a lateral plane, though vertical deflections were observed in many cases before the buckling took place finally in lateral direction. Numata observed in his model tests published originally in 1957 that the rails moved spatially in buckling. It was noticed that the initial vertical imperfection had a significant effect on the buckling strength. In this tests Numata did not consider similarity law in vertical plane, therefore a effect of weight was neglected and a vertical imperfection showed a excessive effect.

The dominating factors in rail buckling are stiffness of the rail structures and imperfections in vertical and horizontal directions, weight of the system and lateral resistance of ballast. The rail buckles to the weakest direction of course.

Dr. Y. Sato of the Railway Technical Research Institute wrote to the authors that in order to overcome buckling of rail, the vertical buckling is kept down by heavy concrete ties and then the lateral buckling should be controlled by careful maintenance. This is the standpoint of Japanese National Railways.

Kerr presented a paper[7] which reviews and discusses various aspects of railroad track buckling in the vertical plane. He divided the published analysis on this field (vertical track buckling) into two main categories. In one category, the authors assume that the track is an elastic beam which is continuously supported by a Winkler base, before as well as during buckling. In the other group, the authors assume that the track is a beam of uniform weight, which rests on a rigid base and that the buckling load is reached when part of the track lifts itself off the base. Based on the comparison of theoretical buckling mode and the actual buckling mode, Kerr concluded that the assumption of continuous elastic support buckling is not admissible.

The variational formulation by using the principle of virtual displacements[10] was adopted to get a nonlinear governing equation for the thermal buckling of continuous track. From this equation, a temperature vs. equilibrating displacement curve is derived up to large deflection phase. The lower limit of temperature increase of this curve is regarded as the safe temperature increase

* Master of Engineering, Graduate of Asian Institute of Technology.

** Member of JSCE, Professor, Department of Transportation Engineering, Nihon University.

which means that above this minimum temperature increase there can exist lifted up equilibrium configuration.

M. Kawaguchi[3),4)] used theoretical and also experimental methods to study the thermal buckling of pavement which is very similar to the stability problem of the railway track in the vertical plane. Based on the observations in his experiments, he concluded that the buckling of continuous pavement is a kind of the snap-through buckling. On the other words, when the axial force is larger than the lower limit of the buckling load, the system has two equilibrium states with deflection among which the state with larger deflection is a stable solution. He also showed that initial imperfections have significant effect on the actual buckling load.

Kerr's lowest temperature increase or Kawaguchi's lower limit of buckling load is a necessary condition for existence of buckled equilibrium configuration and which is only a conservative estimation of buckling load. Actually, the true buckling load for pavements with initial imperfection is a bifurcation load which has a mechanical meaning. At this bifurcation load the pavements must buckle. H. Meier[11)] suggested uniquely the bifurcation in his analysis.

Although Kerr[10)] and other many researchers on the vertical buckling derived the governing equations and solutions of continuous rails, these formulations did not include the effect of initial imperfections of rails. Moreover, they used the point of lowest temperature increase which seems too conservative in the practice. Therefore, a relation between initial imperfections of rails and the actual critical temperature (instead of the safe temperature increase) is expected to be derived. This relation will be useful in practice in the estimation and prevention of thermal buckling of railway track, although Kerr[6)] introduced that E. Stangi concluded that a criterion of the lowest temperature increase was safer. This is the first target of this paper.

Kerr[9)] summarized a series of published results of track buckling tests in lateral plane. In tests, when the buckling loads were reached the rail-tie structures first lifted off from the ballast, stayed in this position for a short while, and then fell sideways to the ground. For this kind of buckling, a slight lift-off is sufficient to eliminate the part of lateral resistance due to ballast, which in turn reduces the safe temperature. To find the mechanism of vertically originated lateral buckling and axial force and corresponding temperature increase of the buckling, is the second target of this paper.

2. BASIC ASSUMPTION

The following assumptions and definitions are made:

(1) The rails of the track are long rails, i.e., the effect of the discontinuity due to the expansion joints can be neglected.

(2) A vertical initial imperfection $w_0(x)$ exists along the rail, as shown in **Fig. 1(a)**.

The amplitude of the initial imperfection h is small compared with the length of the imperfectin region $2l$.

(3) A higher buckling mode requires a larger buckling load, and the unsymmetric buckling mode is not reasonable[1)]. Thus, we assume the vertical buckling mode of lift-off region as shown in **Fig. 1(b)**.

(4) The actual rail-tie structure is replaced by an equivalent beam of uniform cross section, which is symmetrical with respect to vertical z–x plane. The x-axis is placed through the centroid of the cross-section and is chosen as the reference axis.

(5) It is assumed that the track is subjected to a uniform temperature change and a uniformly distributed weight q per unit length of track axis. The track weight q consists of the unit weight of two rails, the average weight of cross-ties and fasteners per unit length of track.

(6) Under sufficiently large values of P, the buckling of the track occurs.

Buckling is assumed to occur in the vertical plane first.

(7) Then in the lift-off region of length $2L$, part of the constrained thermal expansions is released. This results in a reduction of the axial force to P_a, which is assumed to be constant in entire lift-off region.

(8) The base of the track is rigid; the rails respond elastically before and during buckling.

(9) The strains and deformations of rails are relatively small. Plane cross section before buckling remains plane after buckling. Shearing deformations are neglected.

(10) At the instant of vertical buckling, the buckling length is assumed to be equal to the length of initial imperfection and the equation of displacement at $x=0$, equal to initial imperfection[1)].

(11) After vertical buckling, a slight lift-off of rail is sufficient to eliminate lateral resistance from ballast. At the instant of horizontal buckling, the buckling length is assumed to be equal to the length of vertical lift-off region.

3. ANALYSIS AND SOLUTION OF VERTICAL BUCKLING

(1) The Effect of Adjoining Regions

As shown in **Fig. 1**, it is assumed that rails rest on a "rigid" base. Because of a uniform temperature increase and constrained axial expansions, the rails are subjected to an axial compressive force P. For large value of P, the track buckles out vertically and the length of buckling region increases gradually. In the lift-off region of length L, a part of thermal expansion is released, that results in a reduction of axial force to P_a, which is assumed to be constant in the entire lift-off region. In the adjoining regions L_f, the constrained thermal expansions are varied owing to ballast resistance to axial displacements of the track; so are the axial forces $P_a<P_f<P$, where P_f is the axial force in the regions of $L\leq|x|\leq L+L_f$.

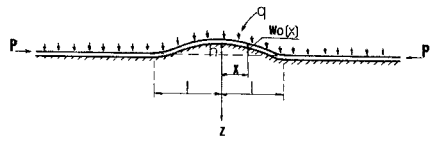

(a) Before buckling; initial imperfection.

$$w_0(x)=-\frac{h}{2}\left(1+\cos\frac{\pi x}{l}\right)$$

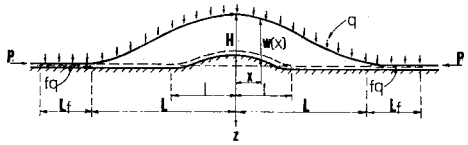

(b) After buckling; deformation.

$$w(x)=-\frac{H}{2}\left(1+\cos\frac{\pi x}{L}\right)$$

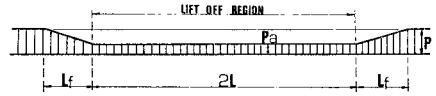

(c) Variation of axial load in post-buckling state.

Fig. 1

According to the above observations, vertical buckling is a local phenomenon, which is observed in a limited area of length $2(L+L_f)$.

The friction force between ballast and rail-tie structures within the regions $L\leq|x|\leq L+L_f$ is assumed to be fq per unit length of rails, where f is friction constant between rail-tie structures and ballast, and q is the unit weight of rail-tie structures. Then, the axial force $P(x)$ of any section in these three regions can be expressed as follows:

$$P(x)=P_a=\text{constant} \quad \text{for } 0\leq|x|\leq L \qquad \cdots\cdots(1\cdot a)$$

$$P(x)=P_f=P_a+fq(x-L) \quad \text{for } L\leq|x|\leq L+L_f \qquad \cdots\cdots(1\cdot b)$$

$$P(x)=AE\alpha T=P=\text{constant} \quad \text{for } |x|\geq L+L_f \qquad \cdots\cdots(1\cdot c)$$

in which T is temperature increase. L_f is the length of the region of the rail affected by axial friction force due to ballast resistance to axial displacement of the track. Therefore L_f can be expressed as:

$$L_f=\frac{P-P_a}{fq} \qquad \cdots\cdots(2)$$

From compatibility condition, if we cut the rail at the outer point of the lift-off region, i.e., $x=\pm L$, the displacements at each side of this opening are equal. Considering the right side of buckled part, the displacements of the rail in the x direction $u(x)$, in the region of $L\leq|x|\leq L+L_f$ can be expressed as:

$$u(x)=-\int_x^{L+L_f}\frac{P-P(\xi)}{AE}d\xi \qquad \cdots\cdots(3)$$

Substituting Eq. (1·b) into Eq. (3) and integrating we obtains

$$u(x)=-\frac{fq(L+L_f-x)^2}{2AE} \qquad \cdots\cdots(4)$$

where

$$L\leq x\leq L+L_f$$

Introducing Eq. (2) into Eq. (4), we obtain the displacement at outer side of $x=L$, as follows:

$$u(L)_o=\frac{(P-P_a)^2}{2AEfq} \qquad \cdots\cdots(5)$$

The displacement at inner side of such a point is due to the change of curvature in the region $x\leq L$ and the reduction of axial force. It can be given by

$$u(L)_i=-\frac{1}{2}\left\{\int_0^L\left[\frac{dw(x)}{dx}\right]^2dx-\int_0^l\left[\frac{dw_0(x)}{dx}\right]^2dx\right\}+\int_0^L\frac{(P-P_a)}{AE}dx \qquad \cdots\cdots(6)$$

where $w(x)$ is the total vertical displacements measured from x axis to the equilibrium position; $w_0(x)$ is the initial imperfection. $w_0(x)$ and $w(x)$ are assumed as follows:

$$w_0(x)=-\frac{h}{2}\left(1+\cos\frac{\pi x}{l}\right) \qquad \cdots\cdots(7)$$

$$w(x)=-\frac{H}{2}\left(1+\cos\frac{\pi x}{L}\right) \qquad \cdots\cdots(8)$$

Introducing Eqs. (7) and (8) into Eq. (6) and integrating, we have

$$u(L)_i=\frac{\pi^2}{16}\left(\frac{H^2}{L}-\frac{h^2}{l}\right)-\frac{P-P_a}{AE}L \quad \cdots\cdots(9)$$

According to the continuity condition, we let $u(L)_o=u(L)_i$, and solving the resulting equation, leads to an equation of P and P_a as:

$$P=P_a+fqL\left[\sqrt{1+\frac{AE\pi^2}{8fqL^2}\left(\frac{H^2}{L}-\frac{h^2}{l}\right)}-1\right] \quad \cdots\cdots(10)$$

(2) Formulation of Vertical Buckling

In order to derive stable equilibrium states, we apply the principle of minimum potential energy.

For the model shown in **Fig. 1 (b)**, the total potential energy consists of strain energy and potential energy. The former is the sum of bending and axial strain energy. We consider a part of long rail as a free body, which is long enough to include any buckling configuration. When the buckling of rail happens, the change of total potential energy during the buckling is expressed as follows:

$$\Pi=U+V \quad \cdots\cdots(11)$$

where

$$U=2\left\{\frac{1}{2}\int_0^l EI\left\{\frac{d^2}{dx^2}[w(x)-w_0(x)]\right\}^2dx+\frac{1}{2}\int_l^L EI\left[\frac{d^2}{dx^2}w(x)\right]^2dx+\int_0^{L_f}\frac{(P_a+fqx)^2}{2EA}dx+\int_0^L\frac{P_a^2}{2AE}dx-\int_0^{L+L_f}\frac{P^2}{2AE}dx\right\} \quad \cdots(12)$$

and

$$V=2\left\{\int_0^L qw(x)dx-\int_0^l qw_0(x)dx+\int_L^{L+L_f}fqu(x)dx\right\} \quad \cdots\cdots(13)$$

where U is the strain energy, and V is the potential energy.

The linearized formulations of beam-column theory are adopted in Eq. (12). That is the curvature is derived by the second derivative of vertical deflection w'' and normal strain at the neutral axis depends on the first derivative of axial displacement u' and a square of the derivative of vertical displacement w'^2 as shown in Eq. (6).

Substituting Eqs. (4), (7), (8) and (10) into Eqs. (11), (12) and (13), then integrating the resulting equation, we obtain

$$\Pi=EI\left\{\frac{H^2\pi^4}{4L^4}\left(\frac{l}{2}+\frac{L}{4\pi}\sin\frac{2\pi l}{L}\right)+S_1+\frac{h^2\pi^4}{8l^3}\right\}+\frac{EIH^2\pi^4}{4L^4}\left(\frac{L}{2}-\frac{l}{2}-\frac{L}{4\pi}\sin\frac{2\pi l}{L}\right)+\frac{P^3-P_a^3}{3AEfq}+\frac{P_a^2L}{AE}-\frac{P^2}{AE}(L_f+L)+q(HL-hl)+\frac{(P-P_a)^3}{3AEfq} \quad \cdots\cdots(14)$$

where

$$S_1=\begin{cases}\dfrac{Hh\pi^3}{2L(l^2-L^2)}\sin\dfrac{\pi l}{L} & \text{for } L\neq l\\ -\dfrac{Hh\pi^4}{4l^3} & \text{for } L=l\end{cases}$$

(3) Determination of Critical Temperature Increase in the Rails

The constrained axial force increases as temperature increases. From the model study and experimental results given in [1, 4, 5], it is expected that there will be a critical axial force of buckling (bifurcation load) corresponding to a certain magnitude of geometrical imperfection. As shown in **Fig. 2**, for $h=0.002$ m, the structure does not deform before the axial force P reaches the critical load. When it reaches this critical value, the rails buckle. The buckling is a kind of snap-through buckling. In other words, there exists two equilibrium configurations as the axial force is equal to the critical buckling force. One of them is the unstable equilibrium configuration with deflections $w(x)$ equal to zero. At the instant of buckling, it also can be assumed that, the buckling length $2L$, is equal to the length of initial imperfection $2l$, i.e., $L=l$. The effect of the buckling length will be considered later in **3.(4)**. These two reasons give the idea of determination of the critical axial force and also the critical tempera-

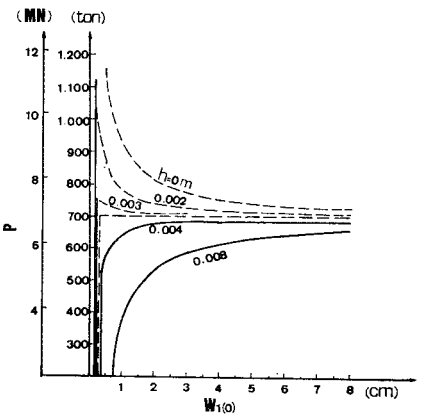

Fig. 2 Axial Force vs. Deformation Curves.

ture increase in the rails. Thus first substituting $L=l$ into Eq. (14), the total potential energy becomes;

$$\Pi=\frac{EI\pi^4}{8l^3}(H^2-2Hh+h^2)-\frac{\pi^2}{8}\left\{\frac{P}{l}(H^2-h^2)-\frac{16f^2q^2l^3}{3AE\pi^2}\left[1+\frac{AE\pi^2}{8fql^3}(H^2-h^2)\right]^{3/2}+fq(H^2-h^2)+\frac{16f^2q^2l^3}{3AE\pi^2}\right\}+ql(H-h) \quad \cdots\cdots(15)$$

According to the principle of stationary total potential energy

$$\frac{\partial\Pi}{\partial H}=0 \quad \cdots\cdots(16)$$

yields the equilibrium equation for $L=l$

$$P=\frac{4l}{\pi^2H}\left\{\frac{EI\pi^4}{4l^3}(H-h)+\frac{\pi^2}{8}\left[2Hfq\left\{1+\frac{AE\pi^2}{8fql^3}(H^2-h^2)\right\}^{1/2}-2Hfq\right]+ql\right\} \quad \cdots\cdots(17)$$

Then, setting the deflection at $x=0$ equal to zero at the instant of buckling, i.e., $H=h$, and substituting it into Eq. (17), we obtain equation of bifurcation load as follows;

$$P_{cr}=\frac{4ql^2}{\pi^2h} \quad \cdots\cdots(18)$$

Once the information of rails, such as unit weight of rail-tie structures q, length of initial imperfection l and initial imperfection h are known, the critical buckling load will be obtained by substituting these into Eq. (18).

As the bifurcation load P_{cr} are determined, the corresponding temperature increase is calculated by

$$T_{cr}=\frac{P_{cr}}{AE\alpha} \quad \cdots\cdots(19)$$

in which α is the coefficient of thermal expansion of rails, and A, E is the cross section and elastic modulus of the rails, respectively.

From **Fig. 2**, it is also of interest to note that P_{cr} diminishes with increasing h and that, for larger imperfection of h, such as $h=0.004$ m there will no snap-through take place at critical load. It may be shown, using the corresponding energy level curves, that in such cases, the deformed equilibrium state is stable. Between the two different kind of buckling configurations, there exists another kind of buckling, i.e., neutral equilibrium configuration. In **Fig. 2**, it can also be seen that all of the linearized solution approach the neutral buckling load asymptotically as the displacements $w_1(0)$ approach infinity.

From Eq. (B·3) in **APPENDIX B**

$$w_1(0)=-\frac{h\lambda^2l^2}{\pi^2-\lambda^2l^2}-\frac{qL}{\lambda^2EI_x}\left(\frac{\cos\lambda L-1}{\lambda\sin\lambda L}+\frac{L}{2}\right) \quad \cdots\cdots(20)$$

in order to obtain P value when $w_1(0)$ approach infinity, we set the first term in Eq. (20) equal to infinity, i.e.,

$$\pi^2-\lambda^2l^2=0 \quad \cdots\cdots(21)$$

where

$$\lambda=\sqrt{\frac{P}{EI_x}}$$

From Eq. (21) we obtain:

$$P_{cr}=\frac{EI_x\pi^2}{l^2} \quad \cdots\cdots(22)$$

which is the Euler buckling load for $q=0$. If we substitute Eq. (22) into Eq. (18), and rewrite the resulting equation, it will yield the corresponding initial imperfection

$$h_{cr}=\frac{4ql^4}{EI_x\pi^4} \quad \cdots\cdots(23)$$

where h_{cr} is a point of demarcation of initial imperfection at which the stable and unstable buckling configuration are divided. For a value of initial imperfection smaller than h_{cr}, the buckling is a sudden snap-through. For those imperfections larger than h_{cr}, the buckling is no longer a snap-through. This idea of h_{cr} was given by Meier[11] first as one of two equilibrium solutions of axial force—vertical displacement equation. However he did not consider the effect of initial imperfection, therefore there was no explanation about a relation between the critical initial imperfection and the unstable solution (with smaller deformation).

(4) Post-Buckling Equilibrium Configuration

The post-buckling equilibrium branch can be obtained by using Eq. (14) and minimizing the total potential energy Π with respect to the unknown parameters. As the authors consider buckling configuration near to the bifurcation point in this paper, they neglect geometrically nonlinear effect of very large deflection after snap-through.

The procedures can be given as follows:

(1) To collect the informations of railroad, such as q, h, l, f, E, A and I_x.

(2) For a certain value of axial force P or temperature T, to assume a certain value of displacement H, starting from the value equal to initial imperfection h.

(3) For each H value, assume a certain value of buckling length L, starting from the length of initial imperfection.

(4) Thus for each set of assumed P, H and L values, the total potential energy Π can be calculated from Eq. (14).

(5) To repeat step (3) and compare the total potential energy, corresponding to each assumed L value, the least value of total potential energy is chosen as the one, corresponding to the certain value of P and H.

(6) To repeat steps (3) to (5) by using several different H values, and connecting those points of minimum total potential energy. An energy level curve corresponding to a certain value of P can be obtained.

(7) To find the points on the energy level curve with a horizontal tangent, corresponding equilibrium configurations.

(8) To repeat steps (2) to (7) and to obtain a corresponding equilibrium branch by correlating those equilibrium configuration.

If we use a track with standard AREA 115 lb/yard rails on wooden crossties, and follow the above procedures, two different kind of buckling configuration will be obtained. The first is as shown in **Fig. 3**. According to the stability criterion, minima on the energy level curves correspond to stable equilibrium configuration, and maxima as well as horizontal inflection points to unstable one. Hence, according to the Π curves of **Fig. 3 (a)** the deformed equilibrium states are unstable until it snap out to a very large deformation. The corresponding equilibrium branch are shown in **Fig. 3(b)**. The second is as shown in **Fig. 4**. The equilibrium branch has two kind of equilibrium. In **Fig. 4 (a)**, each energy level curve has a minimum and a maximum, which are corresponding to a stable and an unstable equilibrium, respectively. In **Fig. 4 (b)**, it also follows that the equilibrium states on the branch AB are stable and those on branch BC are unstable, therefore the axial force at point B is defined as the maximum axial force P_{max}. The lift-off region of length $2L$ does not increase until the buckling load reaches P_{max}. After the point B, the buckling configuration becomes unstable and snaps out. The length $2L$ begins to increase under snap-through displacement.

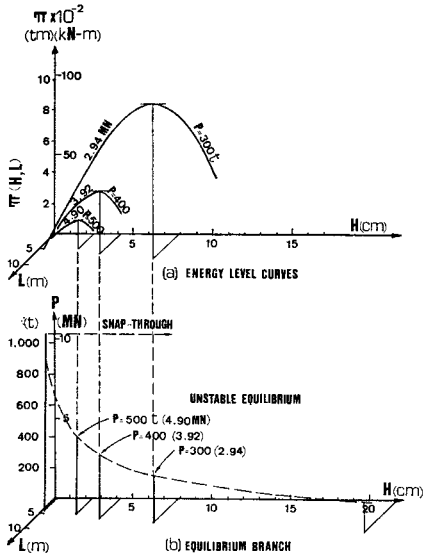

Fig. 3 Energy Level Curves and Corresponding Equilibrium Configuration $l=4$ m, $h=0.002$ m, $E=2.1\times10^7$ t/m^2 (206 gP$_a$), $q=0.35$ t/m (3.43 kN/m), $A=0.0145$ m^2, $I=5.46\times10^{-5}$ m^4.

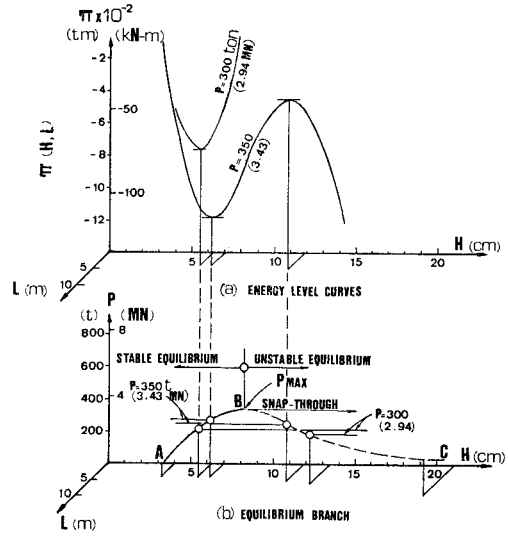

Fig. 4 Energy Level Curves and Corresponding Equilibrium Configuration. Refer to **Fig. 3** for l, E, q, A and I; $h=0.04$ m.

(5) Numerical Example

The following track data are used in numerical calculations.

(1) AREA 115 lb/yard rails on wooden corss-ties

$q=0.35$ t/m (3.43 kN/m),

$E=2.1\times10^7$ t/m^2 (206 GPa),

$I_x=5.46\times10^{-5}$ m^4

$A=0.0145$ m^2, $\alpha=1.05\times10^{-5}$ 1/°C,

$I_y=0.91\times10^{-5}$ m^4

(2) AREA 90 lb/yard rails on wooden crossties
$q=0.2$ t/m (1.96 kN/m),
$E=2.1\times10^{7}$ t/m^2 (206 GPa),
$I_x=3.0\times10^{-5}$ m^4
$A=0.011$ m^2, $\alpha=1.05\times10^{-5}$ 1/°C

(3) JIS 50 kg/m rails on concrete crossties
$q=0.53$ t/m (5.20 kN/m),
$E=2.1\times10^{7}$ t/m^2 (206 GPa),
$I_x=3.48\times10^{-5}$ m^4
$A=0.012\,84$ m^2, $\alpha=1.05\times10^{-5}$ 1/°C,
$I_y=0.754\times10^{-5}$ m^4

(4) JIS 40 kg/m rails on wooden crossties
$q=0.2$ t/m (1.96 kN/m),
$E=2.1\times10^{7}$ t/m^2 (206 GPa),
$I_x=2.756\times10^{-5}$ m^4
$A=0.010\,42$ m^2, $\alpha=1.05\times10^{-5}$ 1/°C,
$I_y=0.46\times10^{-5}$ m^4

(a) For determination of critical temperature increase in the rails, we carry out numerical works on AREA 115 lb/yard and AREA 90 lb/yard rails on wooden crossties with different initial imperfection. We substitute those track data into Eq. (18) and compare the results with the following exact solution which was obtained by solving governing differential equation in **APPENDIX B**. The exact solution is

$$\frac{h\lambda^2l^2}{\pi^2-\lambda^2l^2}+\frac{qL}{\lambda^2EI_x}\left(\frac{\cos\lambda L-1}{\lambda\sin\lambda L}+\frac{L}{2}\right)=0 \qquad \cdots\cdots(24)$$

Table 1 P_{cr} and T_{cr}.

h m	$l=L=3$ m				$l=L=4\frac{1}{2}$m			
	Exact		Approximate		Exact		Approximate	
	P_{cr} (tons) (MN)	T_{cr} (°C)	P_{cr} (tons) (MN)	T_{cr} (°C)	P_{cr} (tons) (MN)	T_{cr} (°C)	P_{cr} (tons) (MN)	T_{cr} (°C)
0.08	16.19 0.159	6.7	15.96 0.157	6.6	28.77 0.282	9.0	28.37 0.278	8.9
0.04	32.37 0.317	13.3	31.92 0.313	13.2	57.51 0.564	18.0	56.74 0.556	17.7
0.02	64.73 0.635	26.7	63.83 0.626	26.3	114.90 1.127	35.9	113.48 1.113	35.5
0.01	129.36 1.269	53.3	127.66 1.252	52.6	229.29 2.249	71.7	226.96 2.226	71.0
0.004	322.73 3.165	133.1	319.16 3.130	131.6	569.17 5.581	178.0	567.40 5.564	177.5
0.002	643.14 6.308	265.2	638.32 6.260	263.2	1 123.15 11.01	351.3	1 134.80 11.13	354.9

* The following data are used in the numerical calculation
$q=0.35$ t/m (3.43 kN/m),
$I=5.46\times10^{-5}$ m^4,
$A=0.0145$ m^2,
$E=2.1\times10^{7}$ t/m^2 (206 GPa),
$\alpha=1.05\times10^{-5}$ 1/C°.

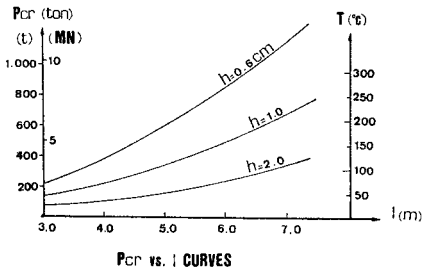

Fig. 5 The Effect of Initial Imperfection Length for Area 115 lb/yard Rail on Wooden Cross-tie. $q=0.35$ t/m (3.43 kN/m), $I_x=5.46\times10^{-5}$ m^4, $E=2.1\times10^{7}$ t/m^2 (206 gP$_a$), $A=0.0145$ m^2, $\alpha=1.05\times10^{-5}$/°C.

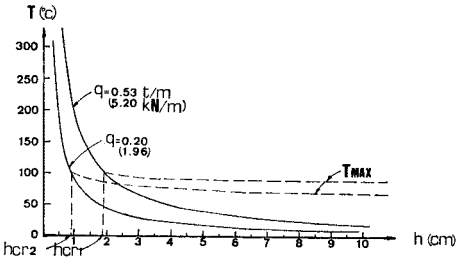

Fig. 6 The Effect of Initial Imperfection with $l=5$ m for 50 kg/m Rail on Concrete Cross-tie ($q=0.35$ t/m, $I_x=3.48\times10^{-5}$ m^4, $A=0.01284$ m^2), 40 kg/m Rail on Wooden Cross-tie ($q=0.20$ t/m, $I_x=2.756\times10^{-5}$ m^4, $A=0.010\,42$ m^2).

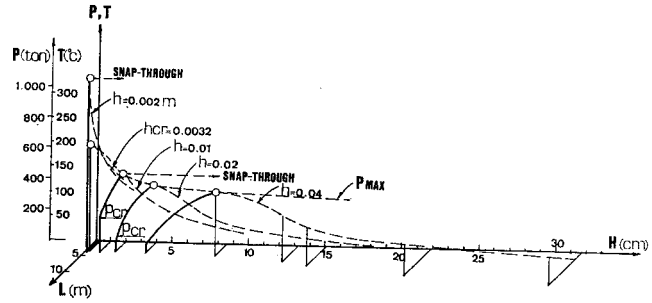

Fig. 7 Post-buckling Equilibrium Branches for Area 115 lb/yard Rail on Wooden Cross-tie with $l=4$ m.

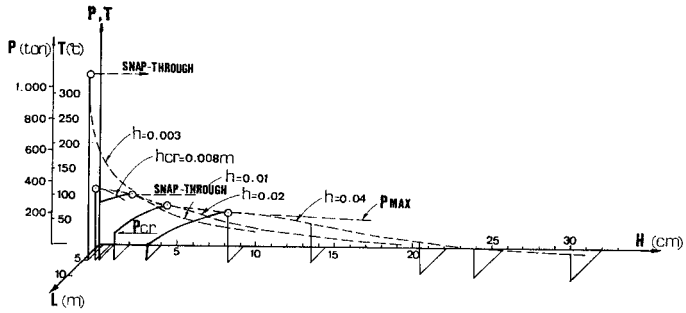

Fig. 8 Post-buckling Equilibrium Branches for Area 115 lb/yard Rail on Wooden Cross-tie with $l=5$ m.

where

$$\lambda=\sqrt{\frac{P_{cr}}{EI_x}}$$

The results are shown in **Table 1** and **Fig. 5**. From the Table it can be concluded that the accuracy of energy method is quite good. And from **Fig. 5** we can realize that the buckling loads decrease with the increasing steepness of slope.

For JIS 50 kg/m rails on concrete crossties and JIS 40 kg/m rails on wooden crossties, with initial imperfection length equal to 5 m, the results from Eq. (18) are shown in **Fig. 6**. It shows that the critical buckling temperature and also the critical buckling axial force of the rails are very sensitive to the existence of initial imperfection of the rails. That is, if an imperfection exists in the rails, the critical buckling temperature of the rails will decrease sharply with increasing imperfection.

(b) For post-buckling equilibrium branches, we carry out numerical works described in 3.4 on AREA 115 lb/yard rails on wooden crossties with initial imperfection length $l=4$ m and 5 m.

The results are shown in **Figs. 7** and **8**. In **Fig. 7** for imperfection smaller than h_{cr}, i.e., $h<$ 0.0032 m, the rail will snap-out suddenly without any warning deflection. For $h>h_{cr}$, the rail will lift off at P_{cr} and force will increase up to $P_{\max}$ with increasing deflections and constant length of the lift-off region, then snap out with increasing length of the lift-off region.

4. ANALYSIS AND SOLUTION OF HORIZONTAL BUCKLING AFTER LIFT OFF VERTICALLY

(1) Formulation of Horizontal Buckling

In most of the track tests[9], when the buckling load reached, the rail-tie structures first lifted off from the ballast, and then fell sideways to the ground. In related tests for the track with German K-type rail fastening devices (wooden or metal ties) the rail-tie structures lifted off the ballast and stayed in this position, apparently because of the higher lateral rigidity of the K-type braced track.

The clarification of this phenomenon that buckling initiates vertically is of importance for the consideration of track stability. If initial imperfection in vertical direction is smaller than h_{cr}, the rail will snapout suddenly in vertical direction. If the vertical imperfection is greater than h_{cr}, the track will start to lift off gradually in vertical direction. This lift-off eliminates a part of lateral resistance due to ballast, therefore

it reduces the safe temperature increase in horizontal direction.

For this kind of buckling, we assume the equation of deflection as follows:

$$v(x)=\sum_{i=1}^{n} C_i\phi_i(x) = \{C_1C_2\}\begin{Bmatrix}\left(1+\cos\frac{\pi x}{L}\right)/2\\ \left(1-\cos\frac{2\pi x}{L}\right)/2\end{Bmatrix} \quad \cdots\cdots(25)$$

where

C_i are indetermined parameters,

ϕ_i are arbitrary functions which are chosen such that $v(x)$ satisfies the kinematic boundary conditions.

The equation of lateral resistance due to ballast at any lifted off position is defined as,

$$k=\begin{cases}\left[1-\frac{H}{2d}\left(1+\cos\frac{\pi x}{L}\right)\right]^2 k_0 & \text{for } 1\geq\frac{H}{d}\geq 0\\ 0 & \text{for } \frac{H}{d}>1\end{cases} \quad \cdots\cdots(26)$$

where k_0 is the lateral resistance of ballast before the rail-tie structure lifted off, and d is the depth of the tie buried in the ballast.

At instant of horizontal buckling, the horizontal buckling length is assumed to be equal to the length of the vertical lift-off region.

When we take the lift-off region as a free body, the total potential energy of the horizontally buckled system is given by

$$\Pi=2\left\{\frac{1}{2}\int_0^L EI_y\left[\frac{d^2v(x)}{dx^2}\right]^2 dx + \frac{1}{2}\int_0^L k[v(x)]^2 dx-\frac{P_h}{2}\int_0^L\left[\frac{dv(x)}{dx}\right]^2 dx\right\} \quad \cdots\cdots(27)$$

Substituting Eqs. (25) and (26) into Eq. (27), yields total potential energy of horizontal buckling in matrix form

$$\Pi=\{c\}^T\left\{\begin{bmatrix}\frac{EI_y\pi^4}{8L^3} & 0\\ 0 & \frac{2EI_y\pi^4}{L^3}\end{bmatrix}+\begin{bmatrix}a_{11} & a_{12}\\ a_{21} & a_{22}\end{bmatrix} -\begin{bmatrix}\frac{P_h\pi^2}{8L} & 0\\ 0 & \frac{P_h\pi^2}{2L}\end{bmatrix}\right\}\{C\} \quad \cdots\cdots(28)$$

where

$$a_{11}=\frac{k_0[F_{11}(L)-F_{11}(xl)]}{4}$$

$$a_{12}=\frac{k_0[F_{12}(L)-F_{12}(xl)]}{4}=a_{21}$$

$$a_{22}=\frac{k_0[F_{22}(L)-F_{22}(xl)]}{4}$$

$$xl=\frac{L}{\pi}\cos^{-1}\left(\frac{2d}{H}-1\right)$$

$$F_{11}(x)=\left[\frac{3}{2}x+\frac{2L}{\pi}\sin\frac{\pi x}{L}+\frac{L}{4\pi}\sin\frac{2\pi x}{L}\right] -\frac{H}{d}\left[\frac{5}{2}x+\frac{4L}{\pi}\sin\frac{\pi x}{L}+\frac{3L}{4\pi} \cdot\sin\frac{2\pi x}{L}-\frac{L}{3\pi}\sin^3\frac{\pi x}{L}\right]+\frac{H^2}{4d^2}\left[\frac{35}{8}x +\frac{8L}{\pi}\sin\frac{\pi x}{L}+\frac{7L}{4\pi}\sin\frac{2\pi x}{L}+\frac{L}{32\pi} \cdot\sin\frac{4\pi x}{L}-\frac{4L}{3\pi}\sin^3\frac{\pi x}{L}\right]$$

$$F_{12}(x)=\left[x+\frac{L}{2\pi}\sin\frac{\pi x}{L}-\frac{L}{2\pi}\sin\frac{2\pi x}{L}-\frac{L}{6\pi} \cdot\sin\frac{3\pi x}{L}\right]-\frac{H}{d}\left[\frac{5}{4}x+\frac{L}{\pi}\sin\frac{\pi x}{L} -\frac{L}{2\pi}\sin\frac{2\pi x}{L}-\frac{L}{3\pi}\sin\frac{3\pi x}{L}-\frac{L}{16\pi} \cdot\sin\frac{4\pi x}{L}\right]+\frac{H^2}{4d^2}\left[2x+\frac{2L}{\pi}\sin\frac{\pi x}{L} -\frac{L}{2\pi}\sin\frac{2\pi x}{L}-\frac{5}{8\pi}\sin\frac{3\pi x}{L}-\frac{L}{8\pi} \cdot\sin\frac{4\pi x}{L}-\frac{L}{40\pi}\sin\frac{5\pi x}{L}-\frac{L}{3\pi} \cdot\sin^3\frac{\pi x}{L}\right]$$

$$F_{22}(x)=\left[\frac{3}{2}x-\frac{L}{\pi}\sin\frac{2\pi x}{L}+\frac{L}{8\pi}\sin\frac{4\pi x}{L}\right] -\frac{H}{d}\left[\frac{3}{2}x+\frac{L}{2\pi}\sin\frac{\pi x}{L}-\frac{L}{\pi}\sin\frac{2\pi x}{L} -\frac{L}{4\pi}\sin\frac{3\pi x}{L}+\frac{L}{8\pi}\sin\frac{4\pi x}{L}+\frac{L}{20\pi} \cdot\sin\frac{5\pi x}{L}\right]+\frac{H^2}{4d^2}\left[\frac{7}{4}x+\frac{L}{\pi}\sin\frac{\pi x}{L} -\frac{17L}{16\pi}\sin\frac{2\pi x}{L}-\frac{L}{2\pi}\sin\frac{3\pi x}{L} +\frac{L}{4\pi}\sin\frac{4\pi x}{L}+\frac{L}{10\pi}\sin\frac{5\pi x}{L} +\frac{L}{48\pi}\sin\frac{6\pi x}{L}\right]$$

According to the principle of stationary total potential energy

$$\left\{\frac{\partial\Pi}{\partial C}\right\}=0 \quad \cdots\cdots(29)$$

gives the linear homogeneous equilibrium equation in matrix form

$$\begin{bmatrix} \left(\frac{EI_y\pi^4}{8L^3}+a_{11}\right)-\frac{P_h\pi^2}{8I} & a_{12} \\ a_{21} & \left(\frac{2EI_y\pi^4}{L^3}+a_{22}\right)-\frac{P_h\pi^2}{2L} \end{bmatrix} \begin{Bmatrix} C_1 \\ C_2 \end{Bmatrix}=0 \quad \cdots\cdots(30)$$

It is assumed that P_h is a constant while buckling starts horizontally, because only critical load is the target to evaluate and the post-buckling equilibrium is neglected. There exists non-trivial solution only when the determinant of the coefficient matrix of Eq. (30) vanishes, i.e.,

$$\begin{vmatrix} \left(\frac{EI_y\pi^4}{8L^3}+a_{11}\right)-\frac{P_h\pi^2}{8L} & a_{12} \\ a_{21} & \left(\frac{2EI_y\pi^4}{L^3}+a_{22}\right)-\frac{P_h\pi^2}{2L} \end{vmatrix} =0 \quad \cdots\cdots(31)$$

Thus

$$P_h=\frac{8L^2}{\pi^4}\left\{\frac{\pi^2}{8L}\left(\frac{5EI_y\pi^4}{2L^3}+4a_{11}+a_{22}\right)-\left[\frac{\pi^4}{64L^2}\left(\frac{5EI_y\pi^4}{2L^3}+4a_{11}+a_{22}\right)^2-\frac{\pi^4}{4L^2}\left\{\left(\frac{EI_y\pi^4}{8L^3}+a_{11}\right)\left(\frac{2EI_y\pi^4}{L^3}+a_{22}\right)-(a_{12})^2\right\}\right]^{1/2}\right\} \quad \cdots\cdots(32)$$

where a_{11}, a_{12} and a_{22} are the same as expressed in Eq. (28)

In the same way as vertical buckling mode, the horizontal buckling load is as follows:

$$P_{crh}=P_h+fql\left[\sqrt{1+\frac{AE\pi^2}{8fqL^2}\left(\frac{H^2}{L}-\frac{h^2}{l}\right)}-1\right] \quad \cdots\cdots(33)$$

A process of the horizontal buckling are shown in **Figs. 9** and **10**. From the Figures, the rails initially lift off in vertical direction (as shown by solid line). As the vertical deflection of rail increases, the horizontal resistance due to ballast decreases (as shown by dotted line). The different values of d are the initial depth of ties buried in the gravel. At the points of intersection of the solid lines and dotted lines, the horizontal buckling takes place. If the vertical deflection H corresponding to point of intersection is larger than H corresponding to P_{max}, the horizontal buckling will occurre in the midway of vertical snap-through actually.

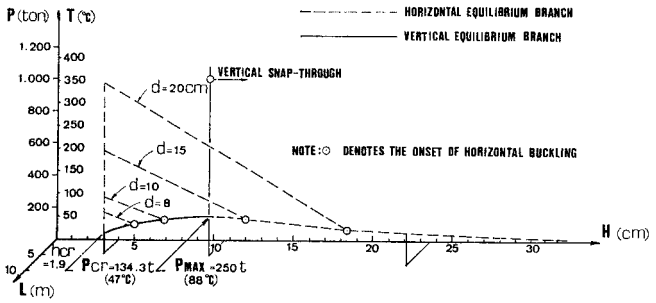

Fig. 9 Post-buckling Equilibrium Branch and the Onset of Horizontal Buckling for 50 kg/m Rail on Concrete Cross-tie with Vertical Initial Imperfection of $h=4$ cm and $l=5$ m.

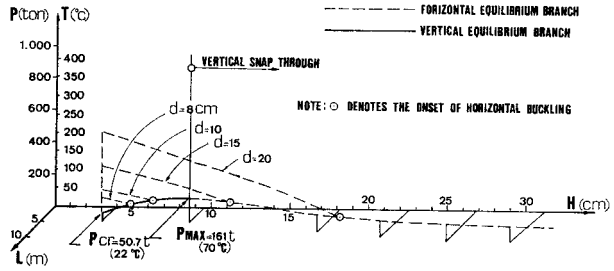

Fig. 10 Post-buckling Equilibrium Branch and the Onset of Horizontal Buckling for 40 kg/m Rail on Wooden Cross-tie with Vertical Initial Imperfection of $h=4$ cm and $l=5$ m.

(2) Numerical Example

The numerical examples are carried out by using following two sets of track data.

50 kg/m Rails on concrete cross-ties		40 kg/m Rails on wooden cross-ties	
$q=0.53$ (5.20)	,	0.2 (1.96)	(t/m) (kN/m)
$I_x=3.48\times10^{-5}$	,	2.756×10^{-5}	(m^4)
$I_y=0.754\times10^{-5}$	,	0.46×10^{-5}	(m^4)
$A=0.012\,84$	,	0.010 42	(m^2)
$E=2.1\times10^7$ (206)	,	2.1×10^7 (206)	(t/m^2) (GPa)
$\alpha=1.05\times10^{-5}$	,	1.05×10^{-5}	(l/°C)
$l=5$	,	5	(m)
$d=0.2$, 0.15, 0.1, 0.08	,	0.2, 0.15, 0.1, 0.08	(m)
$k_0=1\,200$, 675, 300, 192, (11.8, 6.62, 2.94, 1.88),		600, 338, 150, 96 (5.88, 3.31, 1.47, 0.94)	(t/m^2) (MN/m)

The obtained results are shown in **Figs. 9** and **10**. It is obvious that although the reduction of buried depth is small, it may have a profound effect upon the horizontal buckling load. The horizontal buckling temperature increases with increasing buried depth of ties in the ballast.

5. DISCUSSIONS AND CONCLUSIONS

The energy method used in this paper is linearized. Kerr[5] indicated, in a model study of track, that linearized equation gives a P vs w curve which coincides well with the exact P vs w curve when the deflection w is small compared with the length of the lift-off region. It is reasonable therefore to expect that the linearized result in this analysis will agree well with the exact one.

From the results given in **Fig. 3** to **Fig. 10**, the conclusions are derived as follows:

a) Vertical buckling

(1) If the rails are ideally straight, i.e., no initial imperfections exist in the rails, the critical buckling temperature approaches infinity.

(2) The model in **Fig. 1**(a) has a geometric imperfection h. It is assumed that in this state, the system is of no stress. It is anticipated that for large compression force P, equilibrium states exist in which the rail in the region $x\leq\pm L$ does not touch the base neither lifts up. At this moment buckling occurs and the corresponding axial force is called buckling force P_{cr}.

(3) Any small initial imperfections existing in the rails will decrease the critical buckling temperature of the rails significantly. A sharp imperfection of the rails has the lower buckling load than a mild one. The comparison of different length of initial imperfection of rails in **Fig. 5** demonstrates it.

(4) For smaller initial imperfection, the structure does not deform until P reaches the value P_{cr}. At P_{cr}, it snaps out into a strongly deformed equilibrium state. If the imperfection is larger than h_{cr}, the rail starts to lift off at P_{cr} and the axial load will increase gradually with increasing displacement H up to P_{max}, and the length of lift-off region does not increases. After that, a kind of snap-through will take place with increasing lift-off region. The smaller initial imperfection of rails have a higher P_{max} force (as shown in **Figs. 7** and **8**).

(5) The effect of initial imperfection becomes less sensitive as the unit weight of rails q increases. Thus, heavy tracks are more resistive to buckle than the light tracks even they have the same magnitude of initial imperfection.

b) Horizontal buckling after lifted off vertically

(1) The critical temperature increase for horizontal buckling increases with increasing weight of rail-tie structures.

(2) From **Figs. 9** and **10**, it can be seen that the horizontal buckling temperature increases with increasing buried depth of ties in the ballast.

(3) For larger depth of buried ties in the ballast, horizontal buckling occurs in the midway of vertical snap-through. From this, it can be concluded that buckling shall end normally with horizontal buckling configuration, even though buckling initiates vertically. However if horizontal stiffness of the rail-tie structure is increased, the final state will be vertical buckling.

AKNOWLEDGEMENT

This is based on a thesis submitted by the first author in partial fulfilment of the requirements for the degree of Master of Engineering at Asian Institute of Technology. Authors wish to express their sincere gratitude to Dr. Y. Sato and Mr. T. Miyai of Japanese National Railways for their engineering advices.

APPENDIX A: CONCEPT OF POTENTIAL ENERGY FORMULATION

A system shown in **Fig. A** is a simplified model for rail buckling analysis. Deflection curve of member BC is assumed

$$v=v_0\sin\frac{\pi x}{L} \qquad \cdots\cdots(A\cdot1)$$

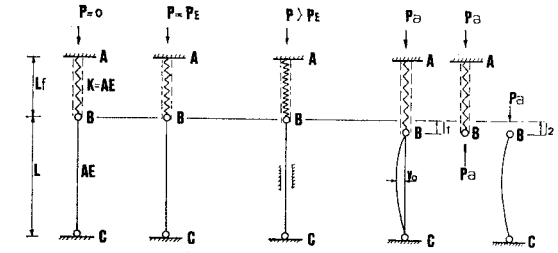

Fig. A

From compatibility condition, the vertical deflection of the member AB at point B is the same as that of the member BC at point B.

$$\Delta l_1=\frac{P-P_a}{K}L_f \quad \cdots\cdots(A\cdot2)$$

$$\Delta l_2=\frac{1}{2}\int_0^L\left(\frac{dv}{dx}\right)^2dx-\frac{(P-P_a)}{AE}L$$

$$=\frac{v_0^2\pi^2}{4L}-\frac{(P-P_a)}{AE}L \quad \cdots\cdots(A\cdot3)$$

$$\Delta l_1=\Delta l_2$$

$$\therefore\quad P_a=P-\frac{v_0^2\pi^2}{4L}\frac{1}{\alpha} \quad \cdots\cdots(A\cdot4)$$

where

$$\alpha=\frac{1}{[L_f/K+L/AE]}$$

The variation in total potential energy of the system is derived in two different ways. At original condition, the axial force is P and v is equal to zero.

Method 1

$$\Pi=\frac{1}{2}\int_0^L EI\left(\frac{d^2v}{dx^2}\right)dx+\frac{P_a^2}{2K}L_f+\frac{P_a^2}{2AE}L$$
$$-\frac{P^2}{2K}L_f-\frac{P^2}{2AE}L \quad \cdots\cdots(A\cdot5)$$

Substituting Eqs. (A·1) and (A.4) into Eq. (A·5), yields

$$\Pi=\frac{EI\pi^4v_0^2}{4L^3}-P\frac{v_0^2\pi^2}{4L}+\left(\frac{v_0^2\pi^2}{4L}\right)^2\frac{1}{2\alpha}$$

Method 2

Take the member B-C as a free body, the variation in total potential energy is given by

$$\Pi=\frac{1}{2}\int_0^L EI\left(\frac{d^2v^2}{dx^2}\right)dx-\int P_a d(\Delta l)\cdots\cdots(A\cdot7)$$

where

$$\Delta l=\frac{1}{2}\int_0^L\left(\frac{dv}{dx}\right)^2dx=\frac{v_0^2\pi^2}{4L}$$

Substituting Eqs. (A·1) and (A·4) into Eq. (A·7) becomes

$$\Pi=\frac{EI\pi^4v_0^2}{4L^3}-P\frac{v_0^2\pi^2}{4L}+\left(\frac{v_0^2\pi^2}{4L}\right)^2\frac{1}{2\alpha} \quad \cdots(A\cdot8)$$

Equations (A·5) and (A·7) give the same results.

The equilibrium equation can be obtained by the principle of stationary total potential energy.

$$\frac{d\Pi}{dv_0}=\frac{EI\pi^4v_0}{2L^3}+\frac{Pv_0\pi^2}{2L}+\frac{v_0^3\pi^4}{8L^2}\frac{1}{\alpha}=0$$
$$\cdots\cdots(A\cdot9)$$

$$P=\frac{EI\pi^2}{L^2}+\frac{v_0^2\pi^2}{4L}\frac{1}{\alpha} \quad \cdots\cdots(A\cdot10)$$

$$\frac{d^2\Pi}{dv_0^2}=\frac{v_0^2\pi^4}{4L^2}\frac{1}{\alpha}>0 \quad \cdots\cdots(A\cdot11)$$

From Eq. (A·11), it can be seen that the system is in a stable equilibrium.

APPENDIX B[1]

The governing equiliblium equation for the buckling of railroad trucks is given as (refer to **Fig. 1**).

In this Appendix w or w_i is measured not from x axis, but from w_0.

$$EIw^{(IV)}+P(w+w_0)''=-r(x)+q(x) \quad \cdots\cdots(B\cdot1)$$

(i) For $0\leq|x|\leq l$, w is denoted by w_1.

$$\omega_0(x)=-\frac{h}{2}\left(1+\cos\frac{\pi x}{l}\right),\quad r(x)=0,\quad q(x)=q$$

(ii) For $l\leq|x|\leq L$, w is denoted by w_2.

$$\omega_0(x)=0,\quad r(x)=0,\quad q(x)=q$$

(iii) For $L\leq|x|$, w is denoted by w_3.

$$\omega_0(x)=0,\quad r(x)=q(x)=q$$

P is assumed constant over the three regions. For the symmetric buckling mode, the boundary conditions are as follows;

$$\left.\begin{aligned}&w_1(\pm l)=w_2(\pm l)\\&w_1'(\pm l)=w_2'(\pm l)\\&w_2(\pm L)=w_2'(\pm L)=0\\&w_3(x)=w_3'(x)=0\end{aligned}\right\} \quad \cdots\cdots(B\cdot2)$$

The solutions are

$$w_1(x)=-\frac{h\lambda^2l^2}{2(\pi^2-\lambda^2l^2)}-\frac{qL}{P}\left(\frac{\cot\lambda L}{\lambda}+\frac{L}{2}\right)$$
$$+\frac{qL}{\lambda P\sin\lambda L}\cos\lambda x+\frac{q}{2P}x^2$$
$$-\frac{h\lambda^2l^2}{2(\pi^2-\lambda^2l^2)}\cos\frac{\pi x}{l} \quad \cdots\cdots(B\cdot3)$$

$$w_2(x)=-\frac{qL}{p}\left(\frac{\cot\lambda L}{\lambda}+\frac{L}{2}\right)+\frac{qL}{p\lambda\sin\lambda L}\cos\lambda x+\frac{q}{2p}x^2 \quad\cdots\cdots(B\cdot4)$$

$$w_3(x)=0 \quad\cdots\cdots(B\cdot5)$$

Substituting $x=0$ into Eq. (B·3), we get Eq. (20). If we set $w_1(0)=0$, Eq. (24) is derived.

LIST OF SYMBOLS

A: area of cross section of the two rails
C_i: parameter for horizontal buckling mode
d: the buried depth of ties in the ballast
E: modulus of elasticity of rails
f: friction constant between rail-tie structures and ballast
H: maximum vertical displacement measured from x-axis
h: maximum vertical height of the initial imperfection of the rails
h_{cr}: a point of demarcation of initial imperfection between stable and unstable buckling configuration
I_x, I_y: moment of inertia of the two rails with respect to the horizontal and vertical centroidal axes, respectively
k: spring constant of lateral resistance due to ballast
k_0: spring constant of lateral resistance due to ballast before lifting off
L: half length of the buckling part of the rails
L_f: the attached region with the existence of axial friction due to ballast
l: half length of the initial imperfection of the rails
P: axial compressive force in the rails due to thermal stress
P_a: axial compressive force in the lift-off portion of rails after vertical buckling occurs
P_{cr}, P_{crh}: critical axial compressive force of rails in vertical and horizontal direction, respectively
P_f: axial compressive force in the region between $L\leq|x|\leq L+L_f$
P_h: critical axial compressive force of horizontal buckling in the lift-off region
P_{max}: maximum axial force in the post-buckling equilibrium branch
$P(x)$: axial compressive force in any section of rails
q: unit weight of rail-tie structures, including two rails, cross-ties and fasteners
T_{cr}: critical temperature increase of rails
T_{max}: the temperature increase in the post-buckling branch corresponds to P_{max}
$u(x)$: the axial displacement in the regions of $L\leq|x|\leq L+L_f$
$w(x),v(x)$: vertical and horizontal displacement function, respectively
$w_0(x)$: imperfection of rails in vertical direction
$w_1(x)$: vertical displacement function measured from $w_0(x)$
X: centroidal axis of the rails
Y,Z: principal axes of the cross-section of the rails
α: coefficient of thermal expansions of the rails
λ: $\sqrt{P/EI_x}$
Π: total potential energy
ϕ_1: arbitrary functions which are chosen so that $v(x)$ satisfies the kinematical boundary conditions.

REFERENCES

1) Chen, L. S.: Thermal Buckling of Long Rail, ST-79-9, Asian Institute of Technology, Bangkok, Thailand.
2) Horikoshi, T.: On the Buckling of Rails, Proceedings of the Japan Society of Civil Engineers, Vol. 20, No. 10, pp. 1187~1227, Oct., 1934 (in Japanese).
3) Kawaguchi, M.: Thermal Buckling of Continuous pavement, Proceedings of the Japan Society of Civil Engineers, No. 170, pp. 331~334, Oct. 1969.
4) Kawaguchi, M.: Snap-Through Buckling of Blocks Laid in a Line, Proc. of JSCE, No. 193, pp. 125~133, Sept., 1971.
5) Kerr, A. D.: A Model Study for Vertical Track Buckling, High Speed Ground Transportation Journal, Vol. 7, No. 3, pp. 351~368, 1973.
6) Kerr, A. D.: The Stress and Stability Analysis of Railroad Tracks, Journal of Applied Mechanics, Transactions of the ASME, pp. 841~848, Dec., 1974.
7) Kerr, A. D.: On the Stability of the Railroad Track in the Vertical Plane, Rail International, pp. 131~142, Feb. 1974.
8) Kerr, A. D.: Buckling of Continuously Supported Beams, Journal of the Engineering Mechanics Division, Proceedings of the ASCE, pp. 247~253, Feb. 1969.
9) Kerr, A. D.: Lateral Buckling of Railroad Tracks due to Constrained Thermal Expansions —A Critical Survey, Proc. Symp. on Railroad Track Mechanics, Pergamon Press, pp. 141~169, 1975.
10) Kerr, A. D.: Determination of Admissible Temperature Increases to Prevent Vertical

Track Buckling, Journal of Applied Mechanics, Transactions of the ASME, pp. 565~573, Sept., 1978.

11) Meier, H.: Einvereinfachtes Verfahren zur Theoretishen Untersuchung der Gleisverwerfung, Organ für die Fortschritte des Eisenbahnwesen, pp. 369~381, Heft 20, 1937 (in Germany)

12) Numata, M.: Buckling Strength of Long Welded Rail, Railway Technical Research Report, No. 721, Aug, 1970, (in Japanese).

(*Received August 21, 1981*)